Syntheses, structures and spectroscopic properties of a novel series of metal–metal bonded complexes Ru(E)(E')(CO)₂(ⁱPr–DAB): (E = Br, E' = Mn(CO)₅; E = SnPh₃, E' = Mn(CO)₅, Re(CO)₅, Co(CO)₄; E = Me, E' = Re(CO)₅; E = E' = Mn(CO)₅, Re(CO)₅; ⁱPr–DAB = N,N'-diisopropyl-1,4-diaza-1,3-butadiene)

Maxim P. Aarnts [a], Ad Oskam [a], Derk J. Stufkens [a,*], Jan Fraanje [b], Kees Goubitz [b], Nora Veldman [c], Anthony L. Spek [c]

[a] Anorganisch Chemisch Laboratorium, J.H. van 't Hoff Research Institute, Universiteit van Amsterdam, Nieuwe Achtergracht 166, 1018 WV Amsterdam, Netherlands
[b] Amsterdam Institute for Molecular Studies, Universiteit van Amsterdam, Nieuwe Achtergracht 166, 1018 WV Amsterdam, Netherlands
[c] Bijvoet Center for Biomolecular Research, Vakgroep Kristal- en Structuurchemie, Universiteit Utrecht, Padualaan 8, NL 3584 CH Utrecht, Netherlands

Abstract

This article describes the syntheses, structures and spectroscopic (IR, Raman, NMR, visible absorption) properties of novel metal–metal bonded complexes of the type *trans,cis*-Ru(E)(E')(CO)₂(ⁱPr–DAB) in which E = Br, Me, SnPh₃, Mn(CO)₅ or Re(CO)₅ and E' = Mn(CO)₅, Re(CO)₅ or Co(CO)₄ (depending on E). The structures of Ru(SnPh₃)(Mn(CO)₅)(CO)₂(ⁱPr–DAB) Ru(SnPh₃)(Co(CO)₄)(CO)₂(ⁱPr–DAB) and Ru(Re(CO)₅)₂(CO)₂(ⁱPr–DAB) were determined by single crystal X-ray diffraction. The complexes have a distorted octahedral geometry with E and E' in axial positions. The structure of Ru(SnPh₃)(Co(CO)₄)(CO)₂(ⁱPr–DAB) is noteworthy, since one of the carbonyl ligands of the Co(CO)₄ group forms a semi-bridge with Ru. The IR and Raman spectra in the ν(CO) and νₛ(CN) wavenumber region are assigned. The absorption spectra show one or two charge-transfer bands in the visible region, their position and number depending on E and E'. The SnPh₃-complexes show in the ¹H NMR spectra a large ⁴J(¹¹⁷/¹¹⁹Sn,H) coupling constant for the imine protons of their ⁱPr–DAB ligands, which points to a strong delocalisation of charge within these complexes.

Keywords: Diimine; Manganese; Carbonyl; Ruthenium; Rhenium; Cobalt

1. Introduction

Much attention has been paid recently to α-diimine-substituted carbonyls [Re(L)(CO)₃(α-diimine)]ⁿ⁺ (n = 0, 1) (α-diimine = bpy, etc.) since they possess rather long lived and stable lowest metal-to-ligand charge transfer (MLCT) states [1–10]. These complexes may undergo inter- and intramolecular energy and electron transfer processes [2,3,11–21], and their emission properties can be influenced by subtle variation of both the α-diimine ligand and the axial ligand L [22]. Photoreactions occur for those complexes in which L is a ligand

or metal fragment that is bound covalently to the metal by a relatively high-energy σ-orbital. Examples are the metal–metal bonded complexes Re(M'Lₙ)(CO)₃(α-diimine) (M'Lₙ = Mn(CO)₅ [23,24], Re(CO)₅ [25], SnPh₃ [26–28], Co(CO)₄ [29], Fe(CO)₂Cp [30]) and the metal–alkyl compounds Re(R)(CO)₃(α-diimine) [31–35]. In addition to the MLCT states these complexes possess a reactive ³σπ* state from which they normally decompose into radicals by homolytic cleavage of the metal–metal or metal–alkyl bond. In the case of the Re(R)(CO)₃(α-diimine) complexes, we have recently studied in detail the mechanism of this homolysis reaction [22,32] and obtained structural information about the ³σπ* state of one of these complexes from its nanosecond time-resolved IR spectra [36].

---

* Corresponding author.

Using the closely related Ru-complexes Ru(X)(R)(CO)$_2$(α-diimine) (X = halide; R = alkyl) as a starting material, a much larger series of complexes can be synthesised since both X and R can be varied. Thus, we have been able to prepare a series of novel inorganometallic complexes Ru(E)(E')(CO)$_2$(^{i}Pr–DAB) in which E and E' represent among others Cl, SnPh$_3$; Me, SnPh$_3$; SnPh$_3$, SnPh$_3$ or PbPh$_3$, PbPh$_3$ and ^{i}Pr–DAB = N,N'-diisopropyl-1,4-diaza-1,3-butadiene) [37]. Those complexes which appeared to be of most interest were those in which both axial ligands (E and E') were an ER$_3$ (E = Ge, Sn, Pb) group. Both the HOMO and LUMO are then strongly delocalised over the axial ligands, as evidenced by the ^{1}H NMR spectrum of, for example, Ru(SnPh$_3$)$_2$(CO)$_2$(^{i}Pr–DAB) and the ESR spectrum of its anion [37,38]. As a result of this delocalisation, the lowest-energy transition of Ru(SnPh$_3$)$_2$(CO)$_2$(^{i}Pr–DAB) can no longer be described as d$_{\pi(Ru)} \rightarrow \pi^*_{(DAB)}$ (MLCT). It is instead a $\sigma_{(Sn-Ru-Sn)} \rightarrow \pi^*_{(DAB)}$ transition which, after intersystem crossing, leads to the occupation of a lowest $^3\sigma\pi^*$ excited state. This latter state is much longer lived (a factor of 1000) [39] than the ^{3}MLCT state of, for example, Ru(Cl)(Me)(CO)$_2$(^{i}Pr–DAB) [40]. These results clearly show that the lifetime of a lowest charge transfer (CT) excited state can appreciably be lengthened by such a delocalisation of charge. Meyer and coworkers observed a similar effect when the charge was delocalised over the α-diimine ligand [41]. In that case the effect of delocalisation was, however, partly offset by a decrease of lifetime caused by a lowering of excited state energy. In order to further investigate the influence of delocalisation of charge over a larger metal fragment, we have synthesised a novel series of di- and trinuclear complexes Ru(E)(E')(CO)$_2$(^{i}Pr–DAB) with E = Br, E' = Mn(CO)$_5$; E = SnPh$_3$, E' = Mn(CO)$_5$, Re(CO)$_5$, Co(CO)$_4$; E = Me, E' = Re(CO)$_5$; E = E' = Mn(CO)$_5$, Re(CO)$_5$. The preparations, structures and some spectroscopic properties of these complexes are described in this article. A more detailed description of their ground- and excited-state properties will be published separately.

2. Experimental section

2.1. Materials

Ru$_3$(CO)$_{12}$, Mn$_2$(CO)$_{10}$, Re$_2$(CO)$_{10}$, Co$_2$(CO)$_8$, SnClPh$_3$ and AgOtf (Otf = CF$_3$SO$_3^-$) were purchased and used without further purification (metal carbonyls were purchased from Strem, all other chemicals from Acros Chimica, unless stated otherwise). The ligand N,N'-diisopropyl-1,4-diaza-1,3-butadiene (^{i}Pr–DAB) was synthesised by literature methods [42]. Chemicals

and solvents for synthetic purposes were of reagent grade, the solvents were freshly distilled from sodium wire (THF, hexane) or CaH$_2$ (CH$_3$CN) and stored under nitrogen atmosphere prior to use. Silicagel (kieselgel 60, Merck, 70–230 mesh) for column chromatography was dried and activated by heating overnight in vacuo at 160 °C. All preparations and purifications were performed under nitrogen atmosphere using Schlenk techniques.

2.2. Synthesis of Ru(Br)(Mn(CO)$_5$)(CO)$_2$(^{i}Pr–DAB)

This complex was prepared by a modified literature method [43]. Ru$_3$(CO)$_{12}$, 0.47 mmol) and ^{i}Pr–DAB (300 mg, 2.14 mmol) were stirred in 50 ml refluxing hexane until a red solution was obtained. When a twofold excess of MnBr(CO)$_5$ (1.2 g, 4.3 mmol) was added to the boiling solution, the complex precipitated immediately as a red solid. After 30 min the solution was cooled to room temperature. The solvent was removed by filtration, and the complex was purified by column chromatography on activated Silica 60, using hexane as the eluent. After the first yellow fraction (MnBr(CO)$_5$) the Ru(Br)(Mn(CO)$_5$)(CO)$_2$(^{i}Pr–DAB) complex was obtained using a hexane–THF mixture in a 7:3 (v:v) ratio as the eluent. The solvent was removed by evaporation in vacuo and the complex was obtained in 50% yield as a red powder.

Ru(Br)(Mn(CO)$_5$)(CO)$_2$(^{i}Pr–DAB). Elemental analysis (%) found (calc.): C = 31.3 (31.5), H = 2.7 (2.8), N = 4.9 (4.9). Mass (FD$^+$): $(m/z)^+$ (int,%) = 574 (100) [M]$^+$. ^{1}H NMR (300.13 MHz, C$_6$D$_6$): δ (ppm) = 7.2 (s, 2H, imine H); 4.38 (sept, 2H, ^3J(H,H) = 6.5 Hz, CH(CH$_3$)$_2$); 1.33 (d, 6H, ^3J(H,H) = 6.5 Hz, CH(CH_3)$_2$ pointing toward Br), 0.75 (d, 6H, ^3J(H,H) = 6.5 Hz, CH(CH_3)$_2$ pointing toward Mn(CO)$_5$). ^{13}C NMR (75.46 MHz, C$_6$D$_6$): δ (ppm) = 203.2 (CO); 155.5 (imine C); 62.6 (CH(CH$_3$)$_2$); 25.1 (CH(CH$_3$)$_2$ pointing toward Br); 22.0 (CH(CH$_3$)$_2$ pointing toward Mn(CO)$_5$).

2.3. Syntheses of Ru(SnPh$_3$)(Mn(CO)$_5$)(CO)$_2$(^{i}Pr–DAB) and Ru(SnPh$_3$)(Co(CO)$_4$)(CO)$_2$(^{i}Pr–DAB)

The complexes were prepared by a modified literature method [44]. To a solution of Mn$_2$(CO)$_{10}$ or Co$_2$(CO)$_8$ (0.5 mmol) in 30 ml THF ca. 0.5 ml sodium–potassium (3:1) alloy was added. The mixture was vigorously stirred until Mn$_2$(CO)$_{10}$ or Co$_2$(CO)$_8$ was completely reduced to Na(K)Mn(CO)$_5$ or Na(K)Co(CO)$_4$ respectively. After removal of the excess Na(K) by filtration (G3), Ru(CF$_3$SO$_3$)-(SnPh$_3$)(CO)$_2$(^{i}Pr–DAB) prepared according to Ref. [37] (1.1 mmol) was added to the solution. The colour of the mixture changed immediately to deep purple. The

reaction mixture was kept in the dark during further manipulations. The solvent was removed by evaporation in vacuo and the complex was purified by column chromatography on activated Silica 60, using hexane as an eluent. The complexes were obtained as a deep purple fraction using hexane–THF in an 8:2 (v:v) ratio as the eluent. The solvent was removed by evaporation in vacuo, and the complexes were obtained in 80% yield as light-sensitive purple powders.

Ru(SnPh$_3$)(Mn(CO)$_5$)(CO)$_2$(^{i}Pr–DAB). Mass (FAB$^+$): $(m/z)^+$, (int, %) = 647 (86) [M – Mn(CO)$_5$]$^+$, 619 (41) [M – Mn(CO)$_5$ – CO], 591 (10) [M – Mn(CO)$_5$ – 2(CO)]$_+$, 702 (6) [M – DAB]$^+$. Mass (FAB$^-$): $(m/z)^-$ (int, %) = 994 (1) [M + S*]$^-$, 842 (1) [M]$^-$, 786(1) [M – 2(CO)]$^-$, 647 (5) [M – Mn(CO)$_5$]$^-$, 493 (20) [M – (SnPh$_3$)]$^-$, 195 (98) [Mn(CO)$_5$]$^-$. S = matrix. Mass (FD$^+$): $(m/z)^+$, (int, %) = 842 (100) [M$^+$]. ^{1}H NMR (300.13 MHz, C$_6$D$_6$): δ (ppm) = 7.56 (85% d, 15% dd, $^3J(^{117/119}$Sn,H) = 41.2 Hz, 6H, ortho-SnC$_6$H$_5$); 7.2 (m, 11H, meta/ para-SnC$_6$H$_5$ and imine H); 4.18 (sept, ^3J(H,H) = 6.5 Hz, 2H, CH(CH$_3$)$_2$); 0.79, (d, ^3J(H,H) = 6.5 Hz, 6H, CH(CH$_3$)$_2$ pointing toward Mn(CO)$_5$), 0.70 (d, ^3J(H,H) = 6.5 Hz, 6H, CH(CH$_3$)$_2$ pointing toward SnPh$_3$). ^{13}C NMR (75.46 MHz, C$_6$D$_6$) δ (ppm) = 207.3 (CO); 147.6 (imine C); 143.0 ($^1J(^{117/119}$Sn,C) = 332.0 Hz SnC); 137.7 ($^2J(^{117/119}$Sn,C) = 34.0 Hz SnCC); 128.2 ($^3J(^{117/119}$Sn,C) = 42.3 Hz SnCCC); 128 (SnCCCC); 62.4 (CH(CH$_3$); 25.6 (CH(CH$_3$) pointing toward Mn(CO)$_5$); 23.5 (CH(CH$_3$) pointing toward SnPh$_3$). ^{119}SnNMR (93.181 MHz, C$_6$D$_6$) δ = –49.3 (Sn). Raman (KNO$_3$, λ_{exc} 476.5 nm): 2065 m, 1998 w, 1471 s, 1468 s, 1284 s, 1165 w, 954 s, 836 s, 654 m, 605 m, 490 w, 425 m, 255 m, 196 m cm^{-1}.

Ru(SnPh$_3$)(Co(CO)$_4$)(CO)$_2$(^{i}Pr–DAB). Mass (FAB$^+$): $(m/z)^+$, (int, %) = 647 (86) [M – Co(CO)$_4$]$^+$, 619 (41) [[M – Co(CO)$_4$ – CO)]$^+$, 591 (10) [M – Co(CO)$_4$ – 2(CO)]$^+$. Mass (FAB$^-$): $(m/z)^-$ (int, %) = 818 (2) [M]$^-$, 647 (10) [M – Co(CO)$_4$]$^-$, 493 (20) [M – SnPh$_3$]$^-$, 171 (100) [Co(CO)$_4$]$^-$. ^{1}H NMR (300.13 MHz, THF-d_8): δ (ppm) = 8.23 (85% s, 15% dd, $^4J(^{117/119}$Sn,H) = 11.2 Hz, 2H, imine H); 7.5 (85% dd, 15% ddd, ^3J(H,H) = 5.4 Hz, ^4J(H,H) 2 Hz, $^3J(^{117/119}$Sn,H) = 41 Hz, 6H, ortho-SnC$_6$H$_5$); 7.3 (m, 9H, meta/para-SnC$_6$H$_5$); 4.12 (sept, ^3J(H,H) = 6.5 Hz, 2H, CH(CH$_3$)$_2$); 1.17 (d, ^3J(H,H) = 6.5 Hz, 6H, CH(CH$_3$)$_2$ pointing toward Co(CO)$_4$); 0.88 (d, ^3J(H,H) = 6.5 Hz, 6H, CH(CH$_3$)$_2$ pointing toward SnPh$_3$). ^{13}C NMR (75.46 MHz, THF-d_8): δ (ppm) = 206 (CO); 157.7 (imine C); 143.5 ($^1J(^{117/119}$Sn,C) = 332.0 Hz, SnC); 139.2 ($^2J(^{117/119}$Sn,C) = 34.0 Hz, SnCC); 130.05 ($^3J(^{117/119}$Sn,C) = 43.8 Hz, SnCCC); 130.02 (SnCCCC); 65.9 (CH(CH$_3$); 26.1 (CH(CH$_3$) pointing toward Co(CO)$_4$); 23.5 (CH(CH$_3$) pointing toward SnPh$_3$). ^{119}Sn NMR (93.181 MHz, THF-d_8) δ = –52 (Sn). Raman (KNO$_3$, λ_{exc} 488 nm):2047 w, 1502

vs, 1294 w, 945 vw, 828 vw, 418 vw, 247 vw, 191 vw cm^{-1}.

2.4. Syntheses of Ru(SnPh$_3$)(Re(CO$_5$)(CO)$_2$(^{i}Pr–DAB) and Ru(Me)(Re(CO)$_5$)(CO)$_2$(^{i}Pr–DAB)

To a solution of Ru(Cl)(SnPh$_3$)(CO)$_2$(^{i}Pr–DAB) [37] or Ru(Cl)(Me)(CO)$_2$(^{i}Pr–DAB) [45] (0.5 mmol) in 10 ml THF ca. 0.25 ml Na(Hg) (1%) was added. The mixture was stirred vigorously until the reduction was completed, as was judged by the colour change from orange to deep red. By careful decanting (to remove the excess of Na(Hg), the solution was added to solid ReBr(CO)$_5$ (0.55 mmol). The colour of the mixture changed immediately to deep purple. The reaction mixture was kept in the dark during further manipulations. The solvent was removed by evaporation in vacuo and the complex was purified by column chromatography on activated Silica 60, using hexane as the eluent. The solvent was removed by evaporation in vacuo. Both complexes were obtained in ca. 80% yield as light-sensitive purple powders.

Ru(SnPh$_3$)(Re(CO)$_5$)(CO)$_2$(^{i}Pr–DAB). Mass (FD$^+$) $(m/z)^+$ (int, %) = 974 (100) [M$^+$]. ^{1}H NMR (300.13 MHz, C$_6$D$_6$): δ (ppm) = 7.59 (85% d, 15% dd, $^3J(^{117/119}$Sn,H) = 41.5 Hz, 6H, ortho-SnC$_6$H$_5$); 7.1 (m, 11H, meta/para-SnC$_6$H$_5$ and imine H); 4.25 (sept, ^3J(H,H) = 6.5 Hz, 2H, CH(CH$_3$)$_2$); 0.84, (d, ^3J(H,H) = 6.5 Hz, 6H, CH(CH$_3$)$_2$ pointing toward Re(CO)$_5$), 0.69 (d, ^3J(H,H) = 6.5 Hz, 6H, CH(CH$_3$)$_2$ pointing toward SnPh$_3$).

Ru(Me)(Re(CO)$_5$)(CO)$_2$(^{i}Pr–DAB). Mass (FD$^+$) $(m/z)^+$ (int, %) = 640 (100) [M$^+$]. ^{1}H NMR (300.13 MHz, C$_6$D$_6$): δ (ppm) = 7.22 (s, 2H, imine H); 4.31 (sept, ^3J(H,H) = 6.5 Hz, 2H, CH(CH$_3$)$_2$); 0.93, (d, ^3J(H,H) = 6.5 Hz, 6H, CH(CH$_3$)$_2$ pointing toward Me), 0.76 (d, ^3J(H,H) = 6.5 Hz, 6H, CH(CH$_3$)$_2$ pointing toward Re(CO)$_5$). 0.29 (s, 3H, RuCH$_3$).

2.5. Syntheses of Ru(Mn(CO)$_5$)$_2$(CO)$_2$(^{i}Pr–DAB) and Ru(Re(CO)$_5$)$_2$(CO)$_2$(^{i}Pr–DAB)

To a solution of Ru(I)$_2$(CO)$_2$(^{i}Pr–DAB) [46] (275 mg, 0.5 mmol) in 30 ml THF, 20 ml of a ca. 0.06 M solution of Na(K)Mn(CO)$_5$ or Na(K)Re(CO)$_5$ in THF [47] (see also the synthesis of Ru-(SnPh$_3$)(Mn(CO)$_5$)(CO)$_2$(^{i}Pr–DAB), Section 2.3) was slowly added. In the case of Ru(Mn-(CO)$_5$)$_2$(CO)$_2$(^{i}Pr–DAB) the orange colour of the solution changed immediately to deep purple, for Ru(Re(CO)$_5$)$_2$(CO)(^{i}Pr–DAB) the colour hardly changed. The reaction mixture was kept in the dark during further manipulations. The solvent was removed by evaporation in vacuo and the complex was purified by column chromatography on activated Silica 60, using hexane as an eluent. The complex was obtained as a

deep purple $(Ru(Mn(CO)_5)_2(CO)_2(^iPr–DAB))$ or orange $(Ru(Re(CO)_5)_2(CO)_2(^iPr–DAB))$ fraction using hexane–THF in a 9:1 (v:v) ratio as eluent. The solvent was removed by evaporation in vacuo. The complexes were obtained in 70% yield as light-sensitive purple and orange powders respectively.

$Ru(Mn(CO)_5)_2(CO)_2(^iPr–DAB)$. Elemental analysis (%) found (calc.): C = 34.9 (35.0), H = 2.3 (2.3), N =

3.9 (4.1). Mass (FD$^+$): $(m/z)^+$, (int, %) = 688 (100%) [M]$^+$. ^{1}H NMR (300.13 MHz, C_6D_6): δ (ppm) = 7.26 (s, 2H, imine H); 3.90 (sept, ^3J(H,H) = 6.3 Hz, 2H, $CH(CH_3)_2$); 0.70 (d, ^3J(H,H) = 6.3 Hz, 12H, $CH(CH_3)_2$). ^{13}C NMR (75.46 MHz, C_6D_6): δ (ppm) = 211.1 (CO), 145.8 (t, $^1J(^{14}N, ^{13}C)$ = 3.0 Hz, imine C), 60.5 ($CH(CH_3)_2$), 24.6 ($CH(CH_3)_2$). Raman (KNO$_3$, λ_{exc} 514 nm): 2080 m, 2058 m, 1469 s, 1282 m, 946 m,

Table 1
Crystallographic data and details of the structure determination of $Ru(SnPh_3)(Mn(CO)_5)(CO)_2(^iPr–DAB)$ (A), $Ru(SnPh_3)(Co(CO)_4)(CO)_2(^iPr–DAB)$ (B) and $Ru(Re(CO)_5)_2(CO)_2(^iPr–DAB)$(C)

Compound	A	B	C
Crystal data			
Empirical formula	$C_{33}H_{31}N_2O_7MnRuSn$	$C_{32}H_{31}N_2O_6CoRuSn$	$C_{20}H_{16}N_3O_{12}Re_2Ru$
M_t	842.6	818.5	949.84
Crystal system	orthorhombic	triclinic	monoclinic
Space group	$Pcab$	$P\bar{1}$	$P2_1/m$
a (Å)	18.145(1)	10.498(2)	9.0764(6)
b (Å)	18.146(1)	16.368(2)	16.6983(13)
c (Å)	20.918(1)	20.733(5)	10.0023(8)
α (deg)	—	105.64(2)	—
β (deg)	—	92.65(2)	116.256(5)
γ (deg)	—	100.77(2)	—
V (Å^3)	6887.4(6)	3353(2)	1359.55(19)
Z	8	4	2
Crystal size (mm^3)	$0.40 \times 0.50 \times 0.80$	$0.10 \times 0.15 \times 0.80$	$0.15 \times 0.36 \times 0.50$
D_x (g cm^{-3})	1.63	1.62	2.320
μ (cm^{-1})	128.14 (Cu Kα)	141.0 (Cu Kα)	94.9 (Mo Kα)
$F(000)$ (electrons)	3344	1624	880
Data collection			
Temperature (K)	243	293	150
θ_{min}, θ_{max} (deg)	4.0, −70.3	2.9, −65.0	2.3, 27.5
SET4 θ_{min}, θ_{max} (deg)	40, 41 (23 refl.)	40, 41 (23 refl.)	10.2,13.9 (25 refl.)
λ (Å)	1.5418 (Cu Kα)	1.5418 (Cu Kα)	0.71073 (Mo Kα)
Monochromator	graphite	graphite	graphite
$\Delta\omega$ (deg)	$1.2 + 0.15\tan\theta$	$1.09 + 0.15\tan\theta$	$0.73 + 0.35\tan\theta$
Aperture (mm)	$3.0 + 1.0\tan\theta$	$3.0 + 1.0\tan\theta$	1.96 (hor.) 4.00 (vert.)
Exposure time (h)	82	128	10.7
Linear instability (%)	0	0	0
Reference reflections	032, 200	$01\bar{3}$, $\bar{2}11$	202, $32\bar{1}$, $3\bar{1}2$
Dataset	0;22, 0;22, 0;25	−12;12, 0;19, −24;23	−11;11, 0;21, −12;12
Total data	6540	11388	6822
Total unique data	6540	11388	3219
Observed data	5014 ($I > 2.5\sigma_I$)	8441 ($I > 2.5\sigma_I$)	2915 ($I > 2\sigma_I$)
DIFABS	0.89–1.29	0.74–1.68	0.63, 2.51
Refinement			
Refined parameters	531	513	186
Final $R1$ [a]	0.044	0.068	0.0306
Final Rw [b]	0.0039	0.044	—
Final $wR2$ [c]	—	—	0.0744
w^{-1}	$7.4 + 0.011(\sigma(F_o))^2$ $+ 0.00015/(\sigma(F_o))$	$7.8 + F_o + 0.012 F_o^2$	$1/\sigma^2(F_o)^2 + 0.0428(P)^2$ $+ 0.0656(P)$ [d]
$(\Delta/\sigma)_{av}$, $(\Delta/\sigma)_{max}$	0.02, 0.61	0.03, 0.74	0.001, 0.000
Min., max. resd. dens.	−1.3, 1.0	−1.2, 1.2	−1.18, 1.87

[a] $R = (\sum_h ||F_o^h| - k|F_c^h||)/(\sum_h |F_o^h|)$.

[b] $R_w = (\sum_h w_h \Delta F_h^2)/(\sum_h w_h |F_o^h|^2)$.

[c] $wR2 = \left\{ \sum \left[w\left(F_o^2 - F_c^2 \right)^2 \right] / \sum \left[w\left(F_o^2 \right)^2 \right] \right\}^{1/2}$.

[d] $P = [\max(F_o^2, 0) + 2F_c^2]/3$.

827 m, 662 m, 600 s, 485 m, 427 m, 242 m, 176 m cm^{-1}.

Ru(Re(CO)$_5$)$_2$(^{i}Pr–DAB). Elemental analysis (%) found (calc.): C = 25.1 (25.3), H = 1.8 (1.7), N = 2.8 (2.9). MASS (FD$^+$); $(m/z)^+$, (int,%) = 952 (100) [M]$^+$. ^{1}H NMR (300.13 MHz, C$_6$D$_6$): δ (ppm) = 7.32 (s, 2H, imine H); 4.00 (sept, ^3J(H,H) = 6.4 Hz, 2H, CH(CH$_3$)$_2$), 0.74 (d, ^3J(H,H) = 6.4 Hz, 12H, CH(CH_3)$_2$). ^{13}C NMR (75.46 MHz, C$_6$D$_6$) δ (ppm) = 212.7 (CO), 193.0 (CO), 140.6 (t, ^1J(^{14}N,^{13}C) = 2.6 Hz, imine C), 60.6 (CH(CH$_3$)$_2$), 25.1 (CH(CH$_3$)$_2$). Raman (KNO$_3$, λ_{exc} 475.9 nm): 2096 s, 2082 s, 1948 w, 1466 s, 1270 s, 1155 m, 957 m, 832 m, 608 s, 538 w, 505 w, 502 w, 459 m, 428 w, 243 w, 187 m cm^{-1}.

2.6. Crystal structure determination of Ru(SnPh$_3$)-(Mn(CO)$_5$)(CO)$_2$(^{i}Pr–DAB)Ru(SnPh$_3$)(Co(CO)$_4$)-(CO)$_2$(^{i}Pr–DAB) and Ru(Re(CO)$_5$)$_2$(CO)$_2$(^{i}Pr–DAB)

Single crystals of all three complexes were grown in a THF–hexane solution at 4 °C. Data collection of Ru(SnPh$_3$)(Mn(CO)$_5$)(CO)$_2$(^{i}Pr–DAB) and Ru(SnPh$_3$)(Co(CO)$_4$)(CO)$_2$(^{i}Pr–DAB) was performed on an Enraf–Nonius CAD-4 diffractometer with graphite-monochromated Cu Kα radiation and ω–2ϑ scan. Accurate unit-cell parameters were refined by a least squares fitting the setting angles of a set of well-centred reflections. Crystal data and details on data collection and refinement are collected in Table 1. Corrections for Lorentz and polarisation effects were applied. The structure was solved by the Patterson search techniques using DIRDIF91 [48]. The hydrogen atoms were placed in calculated positions. Full-matrix least squares refinement on F was carried out, anisotropic for the non-hydrogen atoms and isotropic for the hydrogen atoms. An empirical absorption correction (DIFABS) [49] was applied, see Table 1. The secondary isotropic extinction coefficient $wR2$ [50,51] refined to $G = 0.064(3)$ for Ru(SnPh$_3$)(Mn(CO)$_5$)-(CO)$_2$(^{i}Pr–DAB) and to 0.04(1) for Ru-(SnPh$_3$)(Co(CO)$_4$)(CO)$_2$(^{i}Pr–DAB). A final difference Fourier map revealed a residual electron density in the vicinity of the heavy atoms, see Table 1. Scattering factors were taken from Cromer and Mann [52], and *International Tables for X-Ray Crystallography* [53] The anomalous scattering of the Sn, Ru, Mn, and Co atoms was taken into account. All calculations were performed with XTAL [54], unless stated otherwise. The asymmetric unit of Ru(SnPh$_3$)(Co(CO)$_4$)(CO)$_2$(^{i}Pr–DAB) contains two independent identical molecules. Matching both molecules, except for the hydrogen atoms, led to an r.m.s. of 0.93 Å^2, the greatest difference occurring in the phenyl group C(21)–C(26).

X-ray data for Ru(Re(CO)$_5$)$_2$(CO)$_2$(^{i}Pr–DAB) were collected at 150 K on an Enraf–Nonius CAD4-T diffractometer on rotating anode (Mo Kα, graphite monochro-

mated). Accurate unit-cell parameters were derived from the SET4 [55] setting angles of 25 reflections in the range $10.2 < \theta < 13.9°$. A total of 6822 reflections were scanned, corrected for absorption with the DIFABS algorithm as implemented in PLATON [56], and averaged ($R_{int} = 0.043$) into a unique set of 3219 reflections. The structure was solved with automated Patterson/Fourier techniques using DIRDIF92 [57] and refined on F^2 by full matrix least squares with SHELXL-93 [58] to a final $R = 0.031$, ($S = 1.11$). Crystal data and details on data

Table 2
Fractional coordinates of the non-hydrogen atoms and equivalent isotropic thermal parameters of Ru(SnPh$_3$)(Mn(CO)$_5$)(CO)$_2$(^{i}Pr–DAB)

Atom	x	y	z	U_{eq} (Å^2)
Sn	0.11754(2)	−0.3529(2)	0.33419(2)	0.0162(2)
Ru	0.10556(2)	−0.33177(2)	0.20889(2)	0.0137(2)
Mn	0.11736(6)	−0.28444(6)	0.07439(5)	0.0232(5)
C(1)	0.0691(4)	−0.4852(4)	0.1913(3)	0.024(3)
C(2)	0.0005(3)	−0.4484(4)	0.1938(4)	0.024(3)
C(3)	0.2010(4)	−0.4816(4)	0.1951(4)	0.030(4)
C(4)	0.2158(6)	−0.5108(7)	0.1280(5)	0.054(6)
C(5)	0.2077(5)	−0.5394(6)	0.2453(5)	0.054(6)
C(6)	−0.0694(3)	−0.3377(4)	0.2077(3)	0.024(3)
C(7)	−0.0989(4)	−0.3424(6)	0.2758(4)	0.045(5)
C(8)	−0.1267(4)	−0.3635(5)	0.1594(4)	0.042(5)
C(9)	0.2024(4)	−0.2952(4)	0.2116(4)	0.032(4)
C(10)	0.0732(4)	−0.2370(4)	0.2246(3)	0.027(4)
C(11)	0.2207(4)	−0.4002(4)	0.3662(3)	0.023(3)
C(12)	0.2886(4)	−0.3787(4)	0.3437(4)	0.030(4)
C(13)	0.3544(4)	−0.4082(5)	0.3679(5)	0.044(5)
C(14)	0.3513(5)	−0.4584(4)	0.4164(4)	0.042(5)
C(15)	0.2836(5)	−0.4802(5)	0.4404(4)	0.048(5)
C(16)	0.2185(5)	−0.4518(5)	0.4152(4)	0.038(4)
C(21)	0.1118(3)	−0.2538(3)	0.3920(3)	0.018(3)
C(22)	0.1680(4)	−0.2376(4)	0.4331(4)	0.036(4)
C(23)	0.1631(5)	−0.1765(5)	0.4741(4)	0.053(5)
C(24)	0.1025(4)	−0.1317(4)	0.4725(4)	0.040(4)
C(25)	0.0452(4)	−0.1474(4)	0.4310(4)	0.033(4)
C(26)	0.0500(4)	−0.2084(4)	0.3923(4)	0.026(4)
C(31)	0.0352(4)	−0.4260(4)	0.37497(3)	0.024(3)
C(32)	−0.0089(5)	−0.4011(4)	0.4242(4)	0.041(5)
C(33)	−0.0634(6)	−0.4461(6	0.4498(5)	0.063(7)
C(34)	−0.0744(6)	−0.5160(6)	0.4253(5)	0.059(6)
C(35)	−0.0314(6)	−0.5409(5)	0.3760(5)	0.051(5)
C(36)	0.0241(5)	−0.4967(4)	0.3525(4)	0.036(4)
C(37)	0.0774(4)	−0.3781(4)	0.0677(3)	0.030(4)
C(38)	0.0228(4)	−0.2471(4)	0.0815(4)	0.032(4)
C(39)	0.1225(4)	−0.2624(4)	−0.0095(3)	0.031(4)
C(40)	0.2121(5)	−0.3222(5)	0.0742(4)	0.041(5)
C(41)	0.1534(5)	−0.1951(4)	0.1029(4)	0.039(4)
N(1)	0.1275(3)	−0.4436(3)	0.1969(2)	0.019(3)
N(2)	0.0010(3)	−0.3781(3)	0.2025(2)	0.016(2)
O(9)	0.2616(3)	−0.2759(4)	0.2132(3)	0.062(4)
O(10)	0.0514(4)	−0.1775(3)	0.2346(3)	0.049(4)
O(37)	0.0511(3)	−0.4341(3)	0.0595(3)	0.039(3)
O(38)	−0.0351(3)	−0.2240(3)	0.0832(3)	0.053(4)
O(39)	0.1269(3)	−0.2471(4)	−0.0627(3)	0.050(4)
O(40)	0.2712(4)	−0.3416(5)	0.0718(4)	0.076(5)
O(41)	0.1764(4)	−0.1398(3)	0.1182(3)	0.067(5)

Table 3
Fractional coordinates of the non-hydrogen atoms and equivalent isotropic thermal parameters of Ru(SnPh₃)(Co(CO)₄)(CO)₂('Pr–DAB)

Atom	x	y	z	U_{eq} (Å²)
Ru(1a)	0.69340(5)	1.18252(3)	0.20859(3)	0.0294(3)
Sn(1a)	0.79737(5)	1.26553(3)	0.33315(2)	0.0358(3)
Co(1a)	0.5147(1)	1.14841(9)	0.09227(7)	0.0439(7)
C(1a)	0.8940(8)	1.0851(5)	0.1808(4)	0.046(5)
C(2a)	0.8015(8)	1.0334(6)	0.2078(4)	0.044(5)
C(3a)	0.9658(9)	1.2166(7)	0.1481(5)	0.055(6)
C(4a)	0.908(1)	1.209(1)	0.0773(6)	0.077(8)
C(5a)	1.102(1)	1.2009(8)	0.1491(9)	0.086(9)
C(6a)	0.5981(9)	1.0118(5)	0.2570(4)	0.044(4)
C(7a)	0.643(1)	0.9429(7)	0.2846(6)	0.069(7)
C(8a)	0.482(1)	0.9720(6)	0.2058(5)	0.053(5)
C(9a)	0.7162(7)	1.9215(5)	0.1925(4)	0.035(4)
C(10a)	0.5314(8)	1.1958(5)	0.2423(4)	0.038(4)
C(11a)	1.0060(8)	1.2847(5)	0.3541(4)	0.039(4)
C(12a)	1.062(1)	1.2532(6)	0.4013(4)	0.053(5)
C(13a)	1.199(1)	1.2685(7)	0.4153(5)	0.066(6)
C(14a)	1.278(1)	1.3153(8)	0.3821(6)	0.066(6)
C(15a)	1.224(1)	1.3459(8)	0.3373(6)	0.072(7)
C(16a)	1.089(1)	1.3328(7)	0.3228(5)	0.062(6)
C(21a)	0.7587(9)	1.3930(5)	0.3723(4)	0.044(5)
C(22a)	0.827(1)	1.4460(6)	0.4328(4)	0.053(5)
C(23a)	0.794(1)	1.5225(7)	0.4671(5)	0.061(6)
C(24a)	0.691(1)	1.5495(7)	0.4395(5)	0.067(7)
C(25a)	0.621(1)	1.4994(7)	0.3795(5)	0.063(6)
C(26a)	0.6583(9)	1.4217(6)	0.3462(4)	0.053(5)
C(31a)	0.7115(9)	1.2096(6)	0.4096(4)	0.051(5)
C(32a)	0.742(1)	1.1358(7)	0.4216(5)	0.065(6)
C(33a)	0.687(1)	1.1056(6)	0.4752(6)	0.076(8)
C(34a)	0.607(1)	1.1502(9)	0.5125(6)	0.078(8)
C(35a)	0.576(1)	1.2212(9)	0.5011(6)	0.074(7)
C(36a)	0.6286(9)	1.2525(7)	0.4496(5)	0.059(6)
C(37a)	0.560(1)	1.1611(8)	0.0138(5)	0.067(7)
C(38a)	0.462(1)	1.2475(7)	0.1205(6)	0.067(7)
C(39a)	0.6248(8)	1.1786(5)	0.0971(4)	0.044(4)
C(40a)	0.365(1)	1.0711(6)	0.0850(5)	0.054(6)
N(1a)	0.8722(7)	1.1591(4)	0.1771(3)	0.040(4)
N(2a)	0.7007(6)	1.0638(4)	0.2281(3)	0.037(3)
O(9a)	0.7380(6)	1.3579(4)	0.1835(3)	0.056(4)
O(10a)	0.4386(6)	1.2055(4)	0.2665(4)	0.062(4)
O(37a)	0.5900(9)	1.1656(7)	−0.0377(4)	0.089(6)
O(38a)	0.4239(9)	1.3099(6)	0.1385(6)	0.108(7)
O(39a)	0.6714(7)	1.0194(4)	0.0784(3)	0.058(4)
O(40a)	0.2692(8)	1.0231(5)	0.0778(4)	0.080(5)
Ru(1b)	1.10447(5)	0.64769(4)	0.20903(3)	0.0320(3)
Sn(1b)	1.02070(5)	0.79477(3)	0.24770(2)	0.0335(3)
Co(1b)	1.2643(1)	0.52903(9)	0.15069(7)	0.0456(8)
C(1b)	0.9326(8)	0.5819(5)	0.2966(4)	0.040(4)
C(2b)	0.8540(8)	0.5590(5)	0.2335(4)	0.038(4)
C(3b)	1.1381(9)	0.6541(6)	0.3648(4)	0.050(5)
C(4b)	1.210(2)	0.583(1)	0.3681(7)	0.10(1)
C(5b)	1.064(1)	0.677(1)	0.4262(6)	0.080(8)
C(6b)	0.8332(8)	0.5624(5)	0.1172(4)	0.040(4)
C(7b)	0.6846(9)	0.5430(8)	0.1192(5)	0.058(6)
C(8b)	0.875(1)	0.4849(6)	0.0701(4)	0.051(5)
C(9b)	1.2760(9)	0.7073(6)	0.2413(5)	0.051(5)
C(10b)	1.1223(8)	0.6720(5)	0.1258(4)	0.041(4)
C(11b)	5.8921(8)	0.8052(6)	0.3273(4)	0.045(5)
C(12b)	0.766(1)	0.7518(7)	0.3198(6)	0.061(6)
C(13b)	0.688(1)	0.7637(9)	0.3733(7)	0.076(8)
C(14b)	0.735(1)	0.827(1)	0.4317(6)	0.082(8)

Table 3 (continued)

Atom	x	y	z	U_{eq} (Å²)
C(15b)	0.854(1)	0.881(1)	0.4398(6)	0.096(9)
C(16b)	0.935(1)	0.8687(8)	0.3878(5)	0.069(7)
C(21b)	1.1640(8)	0.9128(5)	0.2925(4)	0.042(4)
C(22b)	1.263(1)	0.9193(6)	0.3412(5)	0.057(6)
C(23b)	1.3435(9)	0.9980(7)	0.3732(5)	0.058(5)
C(24b)	1.326(1)	1.0724(6)	0.3591(5)	0.059(6)
C(25b)	1.226(1)	1.0685(6)	0.3127(5)	0.061(6)
C(26b)	1.1459(9)	0.9896(6)	0.2797(5)	0.050(5)
C(31b)	0.9197(8)	0.8187(5)	0.1633(4)	0.040(4)
C(32b)	0.7858(9)	0.7887(6)	0.1469(5)	0.049(5)
C(33b)	0.722(1)	0.8021(7)	0.0912(6)	0.070(7)
C(34b)	0.791(1)	0.8481(8)	0.0537(5)	0.074(8)
C(35b)	0.923(1)	0.8784(7)	0.0692(5)	0.061(6)
C(36b)	0.9872(9)	0.8624(6)	0.1226(5)	0.050(5)
C(37b)	1.356(1)	0.6016(8)	0.1101(6)	0.070(7)
C(38b)	1.388(1)	0.5196(9)	0.2076(6)	0.075(8)
C(39b)	1.226(1)	0.4349(7)	0.0796(6)	0.069(7)
C(40b)	1.1232(9)	0.4968(6)	0.1900(4)	0.046(5)
N(1b)	1.0526(6)	0.6265(4)	0.2997(3)	0.038(3)
N(2b)	0.9084(6)	0.5837(4)	0.1853(3)	0.036(3)
O(9b)	1.3787(7)	0.7454(5)	0.2619(4)	0.077(5)
O(10b)	1.1276(7)	0.6884(5)	0.0750(3)	0.061(4)
O(37b)	1.418(1)	0.6466(7)	0.0849(7)	0.120(9)
O(38b)	1.468(1)	0.5085(9)	0.2414(5)	0.129(9)
O(39b)	1.204(1)	0.3750(6)	0.0345(5)	0.116(8)
O(40b)	1.0848(7)	0.4478(4)	0.2069(3)	0.056(4)

collection and refinement are collected in Table 1. All non-hydrogen atoms were refined with anisotropic displacement parameters. Hydrogen atoms were taken into account at calculated positions, riding on their carrier atoms with isotropic displacement parameters derived from the U_{eq} of the atom they were attached to. Fractional coordinates of the non-hydrogen atoms and equivalent isotropic thermal parameters for Ru(SnPh₃)(Mn(CO)₅)(CO)₂('Pr–DAB) Ru(SnPh₃)(Co(CO)₄)(CO)₂('Pr–DAB) and Ru(Re(CO)₅)₂(CO)₂('Pr–DAB) are given in Tables 2–4 respectively. A final difference map did not show residual features ($-1.18 < \Delta\sigma \leftarrow 1.87$ e Å⁻³) other than residual absorption artefacts near Re and Ru. The structure contains voids at $(1/2, 0, 0)$ and $(1/2, 1/2, 0)$. No significant density was found in this volume.

2.7. Spectroscopic measurements

Electronic absorption spectra were recorded on a Perkin–Elmer Lambda 5 UV–vis spectrophotometer provided with a 3600 data station or on a Varian Cary 4E spectrophotometer. Extinction coefficients were determined in triplicate. IR spectra were measured on a BioRad FTS-7 or FTS-A60 FTIR spectrometer equipped with a liquid nitrogen cooled MCT-detector. Resonance Raman (rR) spectra of the samples, prepared as KNO₃ pellets, were measured on a Dilor XY spectrometer with a multichannel diode array detection system. A Spectra

Table 4
Fractional coordinates of the non-hydrogen atoms and equivalent isotropic thermal parameters of $Ru(Re(CO)_5)_2(CO)_2(^iPr-DAB)$

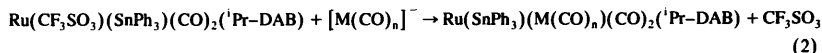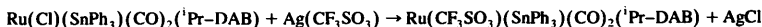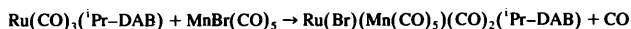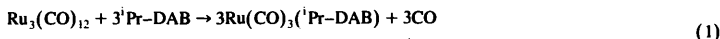| Atom	x	y	z	U_{eq} (Å^2)
Re(1)	0.21447(2)	0.07731(1)	0.34864(2)	0.0172(1)
Ru(1)	0.15674(6)	0.25	0.36179(6)	0.0149(1)
O(9)	0.2467(8)	0.25	0.1058(7)	0.0353(19)
O(10)	0.5176(6)	0.25	0.5760(7)	0.0292(14)
O(27)	0.5269(5)	0.1141(2)	0.3060(5)	0.0382(14)
O(28)	0.4255(6)	0.0780(2)	0.6949(5)	0.0340(12)
O(29)	0.2427(5)	−0.1060(2)	0.3390(5)	0.0330(12)
O(30)	0.0206(6)	0.0899(2)	0.0014(5)	0.0397(14)
O(31)	−0.1079(5)	0.0747(2)	0.3890(6)	0.0332(14)
N(1)	−0.0976(7)	0.25	0.2419(7)	0.0205(16)
N(2)	0.0757(7)	0.25	0.5254(7)	0.0189(16)
C(1)	−0.1799(8)	0.25	0.3215(8)	0.0215(19)
C(2)	−0.0849(8)	0.25	0.4791(8)	0.0219(17)
C(3)	−0.1975(9)	0.25	0.0761(9)	0.030(2)
C(5)	−0.3030(8)	0.1748(4)	0.0224(8)	0.0447(17)
C(6)	0.1777(9)	0.25	0.6891(8)	0.0244(19)
C(7)	0.1499(7)	0.1742(3)	0.7628(6)	0.0314(16)
C(9)	0.2112(9)	0.25	0.2018(9)	0.023(2)
C(10)	0.3802(8)	0.25	0.4922(8)	0.0204(19)
C(27)	0.4162(6)	0.1004(3)	0.3226(6)	0.0242(14)
C(28)	0.3475(7)	0.0787(2)	0.5716(6)	0.0227(14)
C(29)	0.2325(6)	−0.0376(3)	0.3422(6)	0.0231(12)
C(30)	0.0876(7)	0.0859(3)	0.1262(6)	0.0252(16)
C(31)	0.0081(7)	0.0760(2)	0.3716(7)	0.0238(14)

Physics 2016 Ar$^+$ laser was used as the excitation source. To diminish the effect of photodecomposition during the Raman measurement, the pellet was kept spinning and the exciting laser beam was directed on it through a rotating prism. The Raman spectra were corrected for emission of the complexes and recali-

brated for the excitation wavelength-dependent diode array shift using Grams software [59]. ^1H and ^{13}C NMR measurements were carried out on a Bruker AMX 300 spectrometer and ^{119}Sn NMR measurements on a Bruker WM250 spectrometer. Fast atom bombardment (FAB) and field desorption (FD) mass spectra were obtained using a Jeol JMS SX/SX102A four-sector mass spectrometer, coupled to a Jeol MS-MP7000 data system. For FAB the samples were loaded in a matrix solution (nitrobenzylalcohol) onto a stainless steel probe and bombarded with xenon atoms with an energy of 3 keV. For FD, 10 μm tungsten wire FD emitters containing carbon microneedles with an average length of 30 μm were used. The samples were dissolved in methanol–water and then loaded onto the emitters with the dipping technique. An emitter current of 0–15 mA was used to desorb the samples. The ion source temperature was generally 90 °C.

3. Results and discussion

3.1. Synthesis and characterisation

The complex $Ru(Br)(Mn(CO)_5)(CO)_2(^iPr-DAB)$ was prepared according to the reaction in Eq. (1), $Ru(SnPh_3)(M(CO)_n)(CO)_2(^iPr-DAB)$ $(M(CO)_n = Co(CO)_4, Mn(CO)_5)$ according to the reaction in Eq. (2), $Ru(E)(Re(CO)_5)(CO)_2(^iPr-DAB)$ (E = Me, SnPh$_3$) according to the reaction in Eq. (3), and $Ru(M'(CO)_5)_2(CO)_2(^iPr-DAB)$ (M' = Mn, Re) according to the reaction in Eq. (4).

$$Ru_3(CO)_{12} + 3^iPr-DAB \rightarrow 3Ru(CO)_3(^iPr-DAB) + 3CO$$
$$Ru(CO)_3(^iPr-DAB) + MnBr(CO)_5 \rightarrow Ru(Br)(Mn(CO)_5)(CO)_2(^iPr-DAB) + CO \tag{1}$$

$$Ru(Cl)(SnPh_3)(CO)_2(^iPr-DAB) + Ag(CF_3SO_3) \rightarrow Ru(CF_3SO_3)(SnPh_3)(CO)_2(^iPr-DAB) + AgCl$$
$$Ru(CF_3SO_3)(SnPh_3)(CO)_2(^iPr-DAB) + [M(CO)_n]^- \rightarrow Ru(SnPh_3)(M(CO)_n)(CO)_2(^iPr-DAB) + CF_3SO_3 \tag{2}$$

$$Ru(Cl)(E)(CO)_2(^iPr-DAB) + Na(Hg) \rightarrow Na[Ru(E)(CO)_2(^iPr-DAB)] + NaCl$$
$$Na[Ru(E)(CO)_2(^iPr-DAB)] + ReBr(CO)_5 \rightarrow Ru(E)(Re(CO)_5)(CO)_2(^iPr-DAB) + NaBr \tag{3}$$

$$Ru(I)_2(CO)_2(^iPr-DAB) + 2[M'(CO)_5]^- \rightarrow Ru(M'(CO)_5)_2(CO)_2(^iPr-DAB) + 2I^- \tag{4}$$
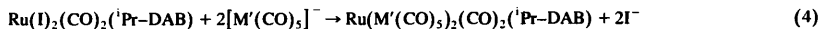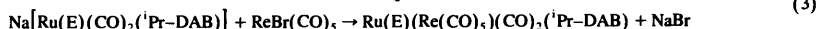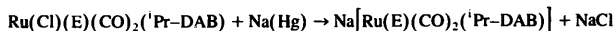
The strongly coloured products are thermally stable and soluble in most common aprotic solvents (hexane, THF, CH$_3$CN, etc.) except for $Ru(SnPh_3)(Co(CO)_4)(CO)_2(^iPr-DAB)$ which decomposes in CH$_3$CN. All complexes are photolabile in solution, but are reasonably photostable as a solid. The complexes are only very slightly air sensitive, except for $Ru(SnPh_3)(Co(CO)_4)(CO)_2(^iPr-DAB)$ and

$Ru(Br)(Mn(CO)_5)(CO)_2(^iPr-DAB)$ which slowly decompose in contact with air. The X-ray structures, visible absorption, IR, Raman, ^1H and ^{13}C NMR data point to the formation of *trans,cis*-$Ru(E)(M(CO)_n)(CO)_2(^iPr-DAB)$, for which the general structure is shown in Fig. 1. These structural and spectroscopic data are reported in the following paragraphs.
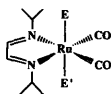
Fig. 1. General structure of *trans,cis*-Ru(E)(E')(CO)$_2$(^{i}Pr–DAB).

3.2. Crystal structures of Ru(SnPh$_3$)(Mn(CO)$_5$)(CO)$_2$-(^{i}Pr–DAB), Ru(SnPh$_3$)(Co(CO)$_4$)(CO)$_2$(^{i}Pr–DAB) and Ru(Re(CO)$_5$)$_2$(CO)$_2$(^{i}Pr–DAB)

ORTEP drawings of the molecular structures of Ru(SnPh$_3$)(Mn(CO)$_5$)(CO)$_2$(^{i}Pr–DAB), Ru(SnPh$_3$)(Co(CO)$_4$)(CO)$_2$(^{i}Pr–DAB) and Ru(Re(CO)$_5$)$_2$(CO)$_2$(^{i}Pr–DAB) are presented in Figs. 2–4 respectively. Selected bond distances and bond angles are collected in Tables 5–7. The general structural data of the three complexes agree well with those of the related complexes Ru(SnPh$_3$)$_2$(CO)$_2$(^{i}Pr–DAB) [38], Ru(Cl)(SnPh$_3$)(CO)$_2$(^{i}Pr–DAB), Ru(Cl)(PbPh$_3$)(CO)$_2$(^{i}Pr–DAB) [37] and Ru(Me)(Mn(CO)$_5$)(CO)$_2$(^{i}Pr–PyCa) [44].

There is, however, a striking difference between the structures of Ru(SnPh$_3$)(Mn(CO)$_5$)(CO)$_2$(^{i}Pr–DAB) and Ru(Re(CO)$_5$)$_2$(CO)$_2$(^{i}Pr–DAB) on the one hand and that of Ru(SnPh$_3$)(Co(CO)$_4$)(CO)$_2$(^{i}Pr–DAB) on the other hand. In all three complexes the metal fragments (Mn(CO)$_5$, Re(CO)$_5$, Co(CO)$_4$) occupy axial positions, but in the Co(CO)$_4$-complex the C(39)–O(39) carbonyl ligand forms a semi-bridge between Co and Ru with a Ru–C(39) bond length of 2.45 Å, (*r*(Ru–C) ≤ 2.28 Å when CO is fully bridging [60]). Secondly, the Ru(SnPh$_3$)(Co(CO)$_4$)(CO)$_2$(^{i}Pr–DAB) crystal consists
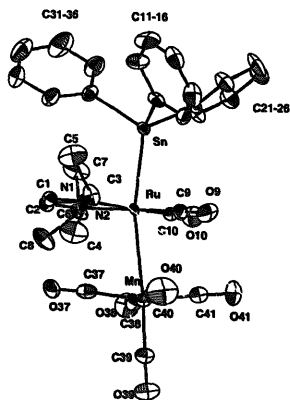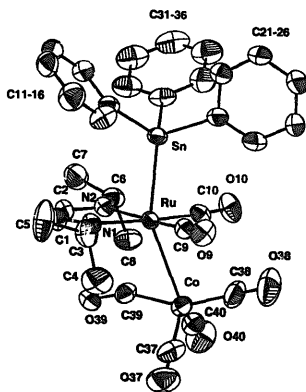

Fig. 3. ORTEP drawing of the non-hydrogen atoms of Ru(SnPh$_3$)(Co(CO)$_4$)(CO)$_2$(^{i}Pr–DAB).

of two independent identical molecules, the main difference being the position of the phenyl group C(21)–C(26). In Fig. 3 only one of the two identical molecules is shown.

The CO ligands of the Mn(CO)$_5$, Co(CO)$_4$ or Re(CO)$_5$ moiety and those of the Ru(CO)$_2$ fragment are in a staggered position with respect to each other (see Figs. 2–4), just as for the Ru(Me)-(Mn(CO)$_5$)(CO)$_2$(^{i}Pr–PyCa) complex [44].

The Ru–M bond lengths of the three complexes are: Ru–Mn = 2.949 Å; Ru–Re = 2.9442 Å; Ru–Co = 2.848 or 2.862 Å. The Ru–Mn bond length agrees well with
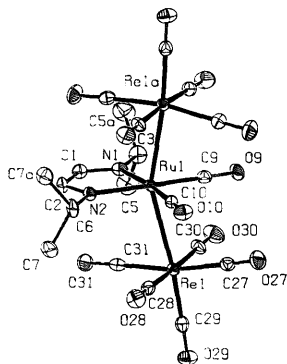

Fig. 2. ORTEP drawing of the non-hydrogen atoms of Ru(SnPh$_3$)(Mn(CO)$_5$)(CO)$_2$(^{i}Pr–DAB).

Fig. 4. ORTEP drawing of the non-hydrogen atoms of Ru(Re(CO)$_5$)$_2$(CO)$_2$(^{i}Pr–DAB).

Table 5
Selected bond distances and angles of Ru(SnPh₃)(Mn(CO)₅)(CO)₂(ᶦPr–DAB) with standard deviations in parentheses

Bond	Distance (Å)/ angle (deg)	Bond	Distance (Å)/ angle (deg)	Bond	Distance (Å)/ angle (deg)
Sn–Ru	2.6579(6)	C(3)–C(5)	1.49(1)	Mn–C(37)	1.853(8)
Ru–Mn	2.949(1)	C(3)–N(1)	1.501(8)	Mn–C(38)	1.852(8)
Ru–C(9)	1.879(7)	C(6)–C(7)	1.52(1)	Mn–C(39)	1.802(7)
Ru–C(10)	1.846(7)	C(6)–C(8)	1.52(1)	Mn–C(40)	1.850(8)
Ru–N(1)	2.083(5)	C(6)–N(2)	1.476(8)	Mn–C(41)	1.847(8)
Ru–N(2)	2.080(5)	C(9)–O(9)	1.130(9)	C(37)–O(37)	1.135(9)
C(1)–C(2)	1.413(9)	C(10)–O(10)	1.168(9)	C(38)–O(38)	1.13(1)
C(1)–N(1)	1.307(8)	Sn–C(11)	2.164(7)	C(39)–O(39)	1.149(9)
C(2)–N(2)	1.288(8)	Sn–C(21)	2.170(6)	C(40)–O(40)	1.13(1)
C(3)–C(4)	1.52(1)	Sn–C(31)	2.171(7)	C(41)–O(41)	1.13(1)
Sn–Ru–Mn	167.64(3)	N(1)–Ru–N(2)	76.9(2)	C(8)–C(6)–N(2)	112.9(6)
Sn–Ru–C(9)	86.8(2)	C(9)–Ru–N(1)	99.7(3)	Ru–N(1)–C(1)	114.7(4)
Sn–Ru–C(10)	89.2(2)	C(9)–Ru–N(2)	176.3(3)	Ru–N(1)–C(3)	128.3(4)
Sn–Ru–N(1)	87.8(1)	C(10)–Ru–N(1)	171.7(3)	C(1)–N(1)–C(3)	116.9(5)
Sn–Ru–N(2)	94.6(1)	C(10)–Ru–N(2)	95.6(3)	Ru–N(2)–C(2)	114.5(4)
Mn–Ru–C(9)	81.8(2)	C(2)–C(1)–N(1)	116.0(6)	Ru–N(2)–C(6)	125.7(4)
Mn–Ru–C(10)	85.5(2)	C(1)–C(2)–N(2)	117.9(6)	C(2)–N(2)–C(6)	119.8(5)
Mn–Ru–N(1)	98.9(1)	C(4)–C(3)–C(5)	112.9(8)	Ru–Mn–C(37)	77.1(2)
Mn–Ru–N(2)	97.0(1)	C(4)–C(3)–N(1)	109.8(6)	Ru–Mn–C(38)	87.9(2)
Ru–C(9)–O(9)	177.3(7)	C(5)–C(3)–N(1)	112.3(6)	Ru–Mn–C(39)	175.7(2)
Ru–C(10)–O(10)	178.7(7)	C(7)–C(6)–C(8)	111.3(6)	Ru–Mn–C(40)	87.8(3)
C(9)–Ru–C(10)	87.9(3)	C(7)–C(6)–N(2)	110.2(6)	Ru–Mn–C(41)	88.5(2)

Table 6
Selected bond distances and angles of Ru(SnPh₃)(Co(CO)₄)(CO)₂(ᶦPr–DAB) with standard deviations in parentheses

Bond	Distance (Å)/angle (deg) [a]		Bond	Distance (Å)/angle (deg) [a]	
Ru–Sn	2.646(1)	2.6509(9)	C(6)–N(2)	1.50(1)	1.51(1)
Ru–Co	2.848(2)	2.862(2)	C(9)–O(9)	1.14(1)	1.14(1)
Ru–C(9)	1.875(9)	1.877(8)	C(10)–O(10)	1.13(1)	1.15(1)
Ru–C(10)	1.897(8)	1.883(9)	Sn–C(11)	2.160(8)	2.171(9)
Ru–C(39)	2.454(7)	2.44(1)	Sn–C(21)	2.147(9)	2.162(7)
Ru–N(1)	2.084(7)	2.080(7)	Sn–C(31)	2.18(1)	2.166(9)
Ru–N(2)	2.102(7)	2.097(6)	Co–C(37)	1.77(1)	1.79(1)
C(1)–C(2)	1.40(1)	1.43(1)	Co–C(38)	1.77(1)	1.80(1)
C(1)–N(1)	1.30(1)	1.32(1)	Co–C(39)	1.79(1)	1.79(1)
C(2)–N(2)	1.29(1)	1.29(1)	Co–C(40)	1.80(1)	1.77(1)
C(3)–C(4)	1.53(2)	1.51(2)	C(37)–O(37)	1.14(2)	1.14(1)
C(3)–C(5)	1.50(2)	1.52(2)	C(38)–O(38)	1.14(2)	1.14(2)
C(3)–N(1)	1.49(1)	1.50(1)	C(39)–O(39)	1.15(1)	1.15(1)
C(6)–C(7)	1.53(2)	1.54(1)	C(40)–O(40)	1.13(1)	1.14(2)
C(6)–C(8)	1.50(1)	1.53(1)			
Sn–Ru–Co	154.94(4)	159.41(4)	C(9)–Ru–N(2)	170.8(3)	173.0(3)
Sn–Ru–C(9)	86.9(2)	90.4(3)	C(10)–Ru–N(2)	97.5(3)	95.2(3)
Sn–Ru–C(10)	85.5(2)	86.0(3)	C(10)–Ru–N(1)	174.3(3)	169.8(3)
Sn–Ru–N(1)	92.5(2)	87.0(2)	C(2)–C(1)–N(1)	118.3(8)	116.8(8)
Sn–Ru–N(2)	89.6(2)	87.4(2)	C(1)–C(2)–N(2)	117.3(9)	116.4(7)
Co–Ru–C(9)	77.9(2)	75.1(3)	Co–C(37)–O(37)	177.0(10)	179.0(10)
Co–Ru–C(10)	75.0(2)	79.9(3)	Co–C(38)–O(38)	178.0(10)	177.0(10)
Co–Ru–N(1)	108.3(2)	108.7(2)	Co–C(39)–O(39)	155.7(7)	154.4(9)
Co–Ru–N(2)	108.1(2)	108.6(2)	Co–C(40)–O(40)	177.0(10)	176.0(10)
Ru–C(9)–O(9)	175.8(7)	178.1(9)	Ru–Co–C(37)	124.2(4)	129.5(4)
Ru–C(10)–O(10)	175.6(7)	176.7(8)	Ru–Co–C(38)	94.2(4)	94.1(4)
C(9)–Ru–C(10)	90.7(3)	91.3(4)	Ru–Co–C(39)	58.7(2)	58.0(3)
N(1)–Ru–N(2)	77.1(3)	77.1(2)	Ru–Co–C(40)	117.7(3)	114.8(4)
C(9)–Ru–N(1)	94.5(3)	96.1(4)			

[a] Crystal consists of two independent identical molecules.

Table 7
Selected bond distances and angles of Ru(Re(CO)$_5$)$_2$(CO)$_2$('Pr–DAB) with standard deviations in parentheses

Bond	Distance (Å)	Bond	Distance (Å)	Bond	Distance (Å)
Re–Ru	2.9442(3)	C(3)–C(5)	1.256(9)	Re–C(29)	1.929(5)
Ru–C(9)	1.872(9)	C(3)–N(1)	1.497(10)	Re–C(30)	2.007(5)
Ru–C(10)	1.864(8)	C(6)–C(7)	1.541(7)	Re–C(31)	1.986(7)
Ru–N(1)	2.078(7)	C(6)–N(2)	1.482(10)	C(27)–O(27)	1.112(8)
Ru–N(2)	2.070(7)	C(9)–O(9)	1.140(1)	C(28)–O(28)	1.118(7)
C(1)–C(2)	1.423(10)	C(10)–O(10)	1.155(10)	C(29)–O(29)	1.147(6)
C(1)–N(1)	1.311(10)	Re–C(27)	1.998(6)	C(30)–O(30)	1.123(7)
C(2)–N(2)	1.320(11)	Re–C(28)	2.012(5)	C(31)–O(31)	1.141(9)
Re–Ru–Re	156.72(2)	N(1)–Ru–N(2)	76.3(3)	Ru–N(1)–C(3)	127.8(5)
Re–Ru–C(9)	80.93(4)	C(9)–Ru–N(1)	98.8(3)	C(1)–N(1)–C(3)	116.4(7)
Re–Ru–C(10)	82.60(4)	C(9)–Ru–N(2)	175.1(3)	Ru–N(2)–C(2)	116.5(5)
Re–Ru–N(1)	98.54(3)	C(10)–Ru–N(1)	173.3(3)	Ru–N(2)–C(6)	127.3(5)
Re–Ru–N(2)	99.66(2)	C(10)–Ru–N(2)	96.0(3)	C(2)–N(2)–C(6)	116.2(7)
Re–Ru–C(9)	80.93(4)	C(2)–C(1)–N(1)	116.4(7)	Ru–Re–C(27)	90.47(15)
Re–Ru–C(10)	82.60(4)	C(1)–C(2)–N(2)	115.0(7)	Ru–Re–C(28)	88.31(10)
Re–Ru–N(1)	98.54(3)	C(4)–C(3)–C(5)	110.8(7)	Ru–Re–C(29)	174.3(2)
Re–Ru–N(2)	99.66(2)	C(4)–C(3)–N(1)	111.6(5)	Ru–Re–C(30)	87.33(15)
Ru–C(9)–O(9)	179.0(8)	C(7)–C(6)–C(8)	110.5(6)	Ru–Re–C(31)	79.05(10)
Ru–C(10)–O(10)	178.2(7)	C(7)–C(6)–N(2)	112.0(4)		
C(9)–Ru–C(10)	88.9(4)	Ru–N(1)–C(1)	115.8(5)		

that in Ru(Me)(Mn(CO)$_5$)(CO)$_2$('Pr-PyCa) (2.9875 Å) [44]. To our knowledge, Ru(Re(CO)$_5$)$_2$(CO)$_2$('Pr–DAB) is the first complex containing a non-bridged Ru–Re bond for which the crystal structure has been determined. Its Ru–Re bond (2.9442 Å) is rather long compared with the Ru–Re bond in the H-bridged (CO)(PPh$_3$)$_2$HRe(μ-H)$_3$RuH(PPh$_3$)$_2$ species (2.59 Å) [61] or in the S-bridged [Re(Ru$_3$)(μ_4-S)(μ-C$_5$H$_4$N)(CO)$_{14}$] complex (2.902 Å) [62]. The Ru–Co bond length is rather short compared with the Ru–Mn or Ru–Re bonds, most probably because of the presence of the semi-bridging CO ligand.

The mean C–O bond lengths of the Ru(CO)$_2$ fragments in Ru(SnPh$_3$)(Mn(CO)$_5$)(CO)$_2$('Pr–DAB) (1.149 Å) and Ru(Re(CO)$_5$)$_2$(CO)$_2$('Pr–DAB)

(1.1475 Å) are slightly longer than those in Ru(SnPh$_3$)(Co(CO)$_4$)(CO)$_2$('Pr–DAB) (1.135 Å), Ru(Cl)(PbPh$_3$)(CO)$_2$('Pr–DAB) (1.13 Å) [37] or Ru(Cl)(SnPh$_3$)(CO)$_2$('Pr–DAB) (1.141 Å) [37]. These differences reflect the different electronic properties of the axial ligands, Mn(CO)$_5$ and Re(CO)$_5$ being more electron releasing than Cl and Co(CO)$_4$. This difference in behaviour is also reflected in the pK_a of the corresponding hydrogen complexes, which decreases in the order HCl ≪ HCo(CO)$_4$ < HMn(CO)$_5$ < HRe(CO)$_5$ [63].

For the DAB skeleton the differences in bond lengths are more subtle. A comparison of the data for Ru(SnPh$_3$)(Mn(CO)$_5$)(CO)$_2$('Pr–DAB), Ru(SnPh$_3$)(Co(CO)$_4$)(CO)$_2$('Pr–DAB) and

Table 8
ν_s(CN) (Raman, KNO$_3$) and ν(CO) (IR, THF) frequencies of Ru(E)(E')(CO)$_2$('Pr–DAB) at room temperature

E	E'	ν_s(CN) (cm^{-1})	ν(CO) (cm^{-1})					
Cl [a]	Cl	—			2050 s		1995 s	
Cl [b]	Me	1568			2024 s		1955 s	
SnPh$_3$ [c]	SnPh$_3$	1473			2005 s		1952 s	
Otf [d]	Mn(CO)$_5$	—		2089 s	2019 s	1994 vs.	1990 sh	
Br	Mn(CO)$_5$	1529 [e]		2074 s	2009 s	1983 vs.	1970 s	
SnPh$_3$	Mn(CO)$_5$	1469		2065 vs.	1994 s	1982 vs.	1967 s	1940 w
Me [f]	Mn(CO)$_5$	1485 [g]		2054 vs.	1992 s	1964 vs.	1948 s	
Mn(CO)$_5$	Mn(CO)$_5$	1469	2082 s	2051 s	2009 s	1991 vs.	1968 s	1918 w
SnPh$_3$	Re(CO)$_5$	—		2087 s	2041 m	1990 vs.	1961 s	1932 w
Me	Re(CO)$_5$	—		2076 s	1987 m	1976 vs.	1952 s	1933 w
Re(CO)$_5$	Re(CO)$_5$	1466	2105 m	2079 s	2020 m	2002 vs.	1968 s	1905 w
SnPh$_3$	Co(CO)$_4$	1502		2048 vs.	2004 s	1978 s		1870 w

[a] From Ref. [68]. [b] From Ref. [45]. [c] From Ref. [37]. [d] Synthesised by reaction of Ru(Br)(Mn(CO)$_5$)(CO)$_2$('Pr–DAB) with Ag(CF$_3$SO$_3$) in THF. [e] Obtained from IR spectrum (KBr). [f] From Ref. [44]. [g] In CH$_2$Cl$_2$.

$Ru(Cl)(SnPh_3)(CO)_2(^iPr-DAB)$ (see Tables 5 and 6 and Ref. [37]) shows that the mean bond lengths of their Ru–N bonds differ. This difference corresponds with the expected variation in π-backdonation caused by the different electronic properties of the axial ligands, as described in the previous paragraph. The C(1)–C(2) bond length shows the same trend, whereas the C(1)–N(1) and C(2)–N(2) bond lengths hardly differ for these complexes. Only the $Ru(Re(CO)_5)_2(CO)_2(^iPr-DAB)$ complex behaves slightly differently with respect to these C=N bonds. The reason for this deviation will be discussed elsewhere [64].

For a few complexes containing an Ru–SnR$_3$ (R = alkyl, aryl) bond the crystal structures have been determined. The Ru–Sn bond length is 2.662 Å in $Ru_3(SnPh_3)(CO)_8H_2(PhHCCPhH)(6Me–pyridine-2-amino-N,N,N')$ [65], 2.603 Å in $Ru(Cl)(SnMe_3)(PPh_3)_2(CO)$ [66], 2.686 Å in $Ru_2(SnMe_3)_2(SnMe_2)_2(CO)_6$ [67], 2.6523 Å in $Ru(Cl)(SnPh_3)(CO)_2(^iPr-DAB)$ [37] and 2.686 Å in $Ru(SnPh_3)_2(CO)_2(^iPr-DAB)$ [38]. The Ru–Sn bonds in $Ru(SnPh_3)(E)(CO)_2(^iPr-DAB)$ (E = $Co(CO)_4$ (2.646 Å); $Mn(CO)_5$ (2.6509 Å)) are within the range of these Ru–SnR$_3$ distances.

3.3. IR and Raman spectra

The IR spectra in the carbonyl stretching region of the complexes under study are collected in Table 8 and representative spectra are depicted in Fig. 5. For comparison Table 8 also contains the IR data of several related complexes and the $\nu_s(CN)$ wavenumbers of the ^iPr-DAB ligand derived from the resonance Raman spectra (vide infra). As can be seen from Table 8, replacement of an electron-withdrawing halide ligand by a more electron-releasing group, such as Me or SnPh$_3$, causes a shift of the $\nu(CO)$ vibrations and of
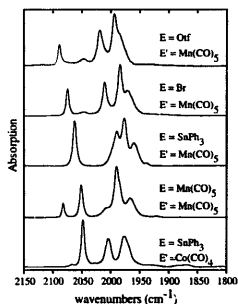

Fig. 5. IR spectra (carbonyl stretching region) of $Ru(E)(E')(CO)_2(^iPr-DAB)$ measured in THF at room temperature.

$\nu_s(CN)$ to smaller wavenumbers. For the complexes not containing a metalcarbonyl group as axial ligand, the highest frequency $\nu(CO)$ vibration was observed as a resonance enhanced band in the Raman spectra [45]. It was accordingly assigned to $\nu_s(CO)$ of the $Ru(CO)_2$ fragment. The low-frequency band then belongs to $\nu_{as}(CO)$.

For the complexes containing an axial metalcarbonyl group ($Mn(CO)_5$, $Re(CO)_5$ or $Co(CO)_4$) assignment of the $\nu(CO)$ bands to vibrations of the separate carbonyl groups is more difficult because of vibrational coupling. It is, however, still possible to establish the predominant character of the bands. Thus, the results of Table 8 show that the axial ligands Me, SnPh$_3$ and $Mn(CO)_5$ do not differ much in their electron-releasing character, since $\nu_s(CN)$ has a rather similar wavenumber for their complexes. In agreement with this, the complexes $Ru(Me)(SnPh_3)(CO)_2(^iPr-DAB)$ and $Ru(SnPh_3)_2(CO)_2(^iPr-DAB)$ also have very similar CO-stretching frequencies [37,39]. If we now compare these $\nu(CO)$ data with those of $Ru(Me)(Mn(CO)_5)(CO)_2(^iPr-DAB)$ and $Ru(SnPh_3)(Mn(CO)_5)(CO)_2(^iPr-DAB)$, we may conclude that the highest-frequency bands, at 2054 and 2065 cm^{-1} respectively, cannot belong to a vibration of the $Ru(CO)_2$ fragment. It is assigned to the highest-frequency vibration of the $Mn(CO)_5$ group. For the closely related complex $Re(Mn(CO)_5)(CO)_3(CO)_3(^iPr-DAB)$ a similar band was observed at 2064 cm^{-1} [69]. In view of the close correspondence between the complexes $Ru(Me)(SnPh_3)(CO)_2(^iPr-DAB)$ [37], $Ru(SnPh_3)_2(CO)_2(^iPr-DAB)$ [37,38], $Ru(Me)(Mn(CO)_5)(CO)_2(^iPr-DAB)$ and $Ru(SnPh_3)(Mn(CO)_5)(CO)_2(^iPr-DAB)$ the two bands of the latter two complexes, at 1992, 1948 cm^{-1} and 1994, 1940 cm^{-1} respectively, are expected to have predominant $Ru(CO)_2$ character. The remaining strong bands of $Ru(SnPh_3)(Mn(CO)_5)(CO)_2(^iPr-DAB)$ at 1982 and 1967 cm^{-1} and the very strong band of $Ru(Me)(Mn(CO)_5)(CO)_2(^iPr-DAB)$ [44] at 1964 cm^{-1} (actually split into two bands at 1973 and 1962 cm^{-1} in hexane) are then tentatively assigned to vibrations of the $Mn(CO)_5$ group. Support for this assignment is provided by comparison with the IR spectra of, for example, $Me_3MMn(CO)_5$ (M = Si, Ge or Sn) [70] with that of $Ru(SnPh_3)(Mn(CO)_5)(CO)_2(^iPr-DAB)$. The former complexes have their main $\nu(CO)$ bands at ca. 2090 and 1990 cm^{-1}. According to the above assignment these vibrations show up at 2065, 1982 and 1967 cm^{-1} in the spectrum of $Ru(SnPh_3)(Mn(CO)_5)(CO)_2(^iPr-DAB)$.

The IR spectrum of $Ru(SnPh_3)(Co(CO)_4)(CO)_2(^iPr-DAB)$ is exceptional in showing a very weak band at 1875 cm^{-1}, which most likely belongs to the vibration of the semi-bridging CO ligand of this complex (see X-ray structure, Section 3.2).

Table 9
Visible absorption maxima (λ_{max}, THF), extinction coefficients ε and solvatochromism ($\Delta = \sigma_{max}(CH_3CN) - \sigma_{max}(hexane)$) of $Ru(E)(E')(CO)_2(^iPr-DAB)$

E	E'	λ_{max} (nm) (ε) ($M^{-1} cm^{-1}$)	Δ (cm^{-1})
Cl [a]	Me	435 (1710)	1870
$SnPh_3$ [b]	$SnPh_3$	515 (6050)	710
Br	$Mn(CO)_5$	401, 507 (7345, 4853)	1077/1233
$SnPh_3$	$Mn(CO)_5$	542 (10980)	440
Me	$Mn(CO)_5$	(13000)	944
$Mn(CO)_5$	$Mn(CO)_5$	467, 554 (13247, 8064)	−185/387
$SnPh_3$	$Re(CO)_5$	524(8269)	327
Me	$Re(CO)_5$	541(14075)	508
$Re(CO)_5$	$Re(CO)_5$	444, 524 (16653, 9278)	−103/146
$SnPh_3$	$Co(CO)_4$	532 (6000)	779 [c]

[a] From Ref. [45]. [b] From Ref. [37]. [c] Decomposes in CH_3CN ($\Delta = \sigma_{max}(THF) - \sigma_{max}(hexane)$).

Fig. 7. UV–vis spectra of $Ru(E)(E')(CO)_2(^iPr-DAB)$ at 293 K in THF.

The rR spectra of all complexes were obtained by excitation into the lowest-energy absorption band. All complexes show resonance enhancement of Raman intensity for a band between 1460 and 1530 cm^{-1} (see Table 8). In agreement with the results from previous rR studies on related ^1Pr-DAB complexes [45,71,72], this band is assigned to $\nu_s(CN)$ of this ligand. There is a clear dependence of the wavenumber of this vibration on the electronic properties of the axial ligands. The complexes $Ru(Br)(Mn(CO)_5)(CO)_2(^iPr-DAB)$ and $Ru(SnPh_3)(Co(CO)_4)(CO)_2(^iPr-DAB)$ have the largest wavenumbers, in agreement with the electron-withdrawing character of Br and $Co(CO)_4$ [63]. Replacement of these ligands by a more electron-releasing $SnPh_3$ or $Mn(CO)_5$ group causes an appreciable shift of $\nu_s(CN)$ to smaller wavenumbers due to the increase of metal to DAB π-backbonding. According to the results from DFT-MO calculations on $Ru(SnH_3)_2(CO)_2(H-DAB)$ [38], this π-backbonding interaction will mainly occur between the $\sigma(E-Ru-E')$ orbital and $\pi^*(^1Pr-DAB)$.

3.4. Electronic absorption spectra

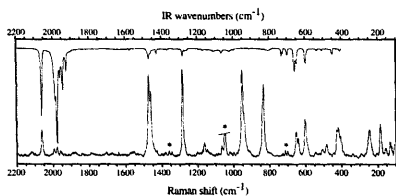The absorption spectra of the complexes under study show one or two bands between 400 and 550 nm,

Fig. 6. IR (KBr) and rR ($^*KNO_3$, $\lambda_{ex} = 476.5$ nm) spectra of $Ru(SnPh_3)(Mn(CO)_5)(CO)_2(^iPr-DAB)$.

depending on the axial ligands. The absorption maxima in this wavelength region are collected in Table 9 and representative spectra are presented in Fig. 6.

In a recent article we demonstrated that the occurrence of two visible absorption bands in the spectra of the complexes $Ru(X)(R)(CO)_3(\alpha\text{-diimine})$ (X = halide, R = alkyl) [45] is caused by the interaction between the Ru d_π and X p_π orbitals. This interaction gives rise to two sets of metal–halide orbitals (bonding and antibonding respectively) from which CT transitions to the lowest π^* orbital of the α-diimine ligand occur. A similar effect has been observed for the complexes fac-$Mn(X)(CO)_3(bpy)$ [73] and $Re(X)(CO)_3(\alpha\text{-diimine})$ [1].

The same interaction between Ru d_π and Br p_π orbitals may be responsible for the presence of the two absorption bands in the spectrum of $Ru(Br)(Mn(CO)_5)(CO)_2(^iPr-DAB)$. The low-energy band then belongs to the CT transitions from the $d_{\pi(Ru)} - p_{\pi(Br)}$ antibonding orbitals to the π^* of the DAB ligand, the higher-energy band to the CT transitions from the corresponding $d_{\pi(Ru)} + p_{\pi(Br)}$ bonding orbitals. In agreement with this assignment only a single absorption band remains when Br is replaced by Me [44] or $SnPh_3$ [37] (Fig. 7). A single absorption band is also observed for the closely related complex $Ru(SnPh_3)(Co(CO)_4)(CO)_2(^iPr-DAB)$. Recent DFT-MO calculations [38] have shown that the lowest-energy absorption band of Ru-complexes having two σ-bonded axial ligands (E, E' = Me, $SnPh_3$, $M(CO)_n$) belongs to the strongly allowed transition from a σ-orbital delocalised over the central atom and the two axial ligands to the lowest π^* orbital of the DAB ligand. It cannot be excluded that such a $\sigma_{(E-Ru-E')} \rightarrow \pi^*_{(DAB)}$ transition also contributes to the intensity of one of the two bands of $Ru(Br)(Mn(CO)_5)(CO)_2(^iPr-DAB)$. The situation becomes more complicated when the bromide is replaced by a second $Mn(CO)_5$ group to give $Ru(Mn(CO)_5)_2(CO)_2(^iPr-DAB)$. The absorption spectrum again shows two bands, the lowest-energy one most probably belonging to a $\sigma_{(Mn-Ru-Mn)} \rightarrow \pi^*_{(DAB)}$

transition. The assignment of the second band is not directly clear, since several CT transitions from delocalised σ- and π-orbitals to $\pi^*_{(DAB)}$ are expected in this wavelength region.

Replacement of Br by the more electron-releasing ligand $SnPh_3$ not only changes the number of bands, the remaining band is also shifted to lower energy. At the same time the negative solvatochromism, i.e. the shift of the absorption maximum to shorter wavelength upon going from the apolar solvent hexane to the polar solvent acetonitrile, decreases. These effects confirm the CT character of the transition(s) which is also evident from the rR effect of $\nu_s(CN)$ (vide supra).

3.5. NMR spectra

The ^1H NMR spectra of the $Ru(E)(E')(CO)_2(^iPr-DAB)$ compounds all show a resonance of the imine protons in the 7.1–8.4 ppm region, which indicates that the ^iPr–DAB ligand is coordinated as σN–$\sigma N'$ chelate [74,75]. The chemical shift of the imine protons is strongly dependent on the electronic properties of the axial ligands. Electron donating ligands ($Re(CO)_5$, $Mn(CO)_5$ or $SnPh_3$) give rise to an up-field shifted imine proton (ca. 8.0 ppm in $CDCl_3$), electron-withdrawing ligands (Br, $Co(CO)_4$) cause a down-field shifted imine proton (ca. 8.3 ppm in $CDCl_3$). In addition, the chemical shift of the imine protons is strongly solvent dependent, as can be seen from Table 10. This strong solvent dependence, which is typical for these types of complex, has already been described in detail [74]. Since not all complexes have a similar solvent dependence, the differences between them are less pronounced in apolar solvents than in the more polar ones. Apparently, the imine proton signal cannot be shifted to lower field than 7 ppm in these two types of complex.

Table 10
Solvent dependence of the chemical shift and $^4J(Sn,H)$ coupling constants of the imine protons of $Ru(E)(E')(CO)_2(^iPr-DAB)$

Complexes		C_6D_6		$CDCl_3$	
E	E'	δ (ppm)	$^4J(Sn,H)$ (Hz)[a]	δ (ppm)	$^4J(Sn,H)$ (Hz)[a]
Br	$Mn(CO)_5$	7.2	—	8.35	—
$SnPh_3$	$Mn(CO)_5$	7.2[b]	—[b]	7.93	16.7
Me[c]	$Mn(CO)_5$	—	—	8.09	—
$Mn(CO)_5$	$Mn(CO)_5$	7.26	—	8.05	—
$SnPh_3$	$Re(CO)_5$	7.2[b]	—[b]	7.91	20.2
Me	$Re(CO)_5$	7.22	—	8.09	—
$Re(CO)_5$	$Re(CO)_5$	7.32	—	7.96	—
$SnPh_3$	$Co(CO)_4$	7.10	10.4	8.23[d]	11.2

[a] Coupling of the imine protons with the $^{117/119}Sn$ isotope. [b] The $^4J(^{117/119}Sn,H)$ coupling constants could only be determined in polar solvents, since the imine signal was obscured by C_6D_6 and phenyl signals of $SnPh_3$ in apolar ones. [c] From Ref. [44]. [d] Broad signal, in THF-d_8 $\delta = 8.23$, $^4J(Sn,H) = 11.2\,Hz$.

Table 11
Chemical shift of the ^iPr-DAB protons of $Ru(E)(E')(CO)_2(^iPr-DAB)(C_6D_6)$

E	E'	$CH(CH_3)_2$	$CH(CH_3)_2$ pointing toward E	$CH(CH_3)_2$ pointing toward E'
Br	$Mn(CO)_5$	4.38	1.33	0.75
$SnPh_3$	$Mn(CO)_5$	4.18	0.70	0.79
$Mn(CO)_5$	$Mn(CO)_5$	3.90	0.70	0.70
$SnPh_3$	$Re(CO)_5$	4.25	0.69	0.84
Me	$Re(CO)_5$	4.31	0.93	0.76
$Re(CO)_5$	$Re(CO)_5$	4.00	0.74	0.74
$SnPh_3$[a]	$Co(CO)_4$	4.12	0.88	1.17

[a] In THF-d_8.

Since the ^iPr-groups of the ^iPr–DAB ligand cannot freely rotate around the C–N axis, two types of Me group can be distinguished, see Table 11. For the methyl groups pointing toward axial ligands, such as Me, Cl, Br, etc., the protons have a chemical shift of approximately 1.3–1.4 ppm [37] (in C_6D_6). The corresponding proton resonance of the methyl groups pointing toward an axial ligand containing a phenyl or carbonyl group is up-field shifted by ca. 0.6 by the influence of the shielding cones of these ligands. The influence of the $SnPh_3$ and $Mn(CO)_5$ ligands upon the methyl groups is almost the same, and the assignment for the $Ru(SnPh_3)(Mn(CO)_5)(CO)_2(^iPr$-DAB) complex is therefore tentative, and only based upon a comparison between the different complexes.

^4J coupling of the imine protons with the $^{117/119}Sn$ nuclei (spin 1/2), were determined for the three Sn-containing complexes. Such coupling constants are a sensitive indicator for the delocalisation of charge within a series of related complexes, as has been shown recently for complexes of the type $Ru(E)(SnPh_3)(CO)_2(^iPr$-DAB) (E = Cl, Me, $SnPh_3$) [37]. For the hardly delocalised complex $Ru(Cl)(SnPh_3)(CO)_2(^iPr$-DAB) $^4J(^{117/119}Sn,H_{imine}) = 8.8\,Hz$ in $CDCl_3$, whereas for the strongly delocalised complex $Ru(SnPh_3)_2(CO)_2(^iPr$-DAB) [38], the $^4J(^{117/119}Sn,H_{imine})$ coupling constant is as high as 26 Hz. The $^4J(^{117/119}Sn,H_{imine})$ value of the $Ru(SnPh_3)(Co(CO)_4)(CO)_2(^iPr$-DAB) complex is comparable with that of the hardly delocalised halide-containing complex $Ru(Cl)(SnPh_3)(CO)_2(^iPr$-DAB), while the $^4J(^{117/119}Sn,H_{imine})$ values of the $Mn(CO)_5$ and $Re(CO)_5$ containing complexes are between those of the strongly delocalised complex $Ru(SnPh_3)_2(CO)_2(^iPr$-DAB) and the hardly delocalised complex $Ru(Cl)(SnPh_3)(CO)_2(^iPr$-DAB). This means that these complexes $Ru(SnPh_3)(M(CO)_5(CO)_2(^iPr$-DAB) (M = Mn, Re) are less delocalised than $Ru(SnPh_3)_2(CO)_2(^iPr$-DAB) and related complexes, or that the $Mn(CO)_5$ and $Re(CO)_5$ groups contribute more to the delocalisation than the $SnPh_3$ ligand.

References

[1] B.D. Rossenaar, D.J. Stufkens and A. Vlek, Jr., *Inorg. Chem.*, 35 (1996) 2902.

[2] D.J. Stufkens, *Comments Inorg. Chem.*, 13 (1992) 359.

[3] K.S. Schanze, D.B. MacQueen, T.A. Perkins and L.A. Cabana, *Coord. Chem. Rev.*, 122 (1993) 63.

[4] A.J. Lees, *Comments Inorg. Chem.*, 17 (1995) 319.

[5] M.S. Wrighton and D.L. Morse, *J. Am. Chem. Soc.*, 96 (1974) 998.

[6] K. Kalyanasundaram, *Proc. Ind. Acad. Sci.*, 104 (1992) 701.

[7] L.A. Lucia, R.D. Burton and K.S. Schanze, *Inorg. Chim. Acta*, 208 (1993) 103.

[8] J.V. Caspar and T.J. Meyer, *J. Am. Chem. Soc.*, 105 (1983) 5583.

[9] L.A. Worl, R. Duesing, P. Chen, L. Della Ciana and T.J. Meyer, *J. Chem. Soc. Dalton Trans.*, (1991) 849.

[10] M.W. George, F.P.A. Johnson, J.R. Westwell, P.M. Hodges and J.J. Turner, *J. Chem. Soc. Dalton Trans.*, (1993) 2977.

[11] P. Chen, R.D. Duesing, D. Graff and T.J. Meyer, *J. Phys. Chem.*, 95 (1991) 5850.

[12] R. Sahai, D.P. Rillema, R. Shaver, S. van Wallendeel, D.C. Jackman and M. Boldaji, *Inorg. Chem.*, 28 (1989) 1022.

[13] S. van Wallendael, R.J. Shaver, D.P. Rillema, B.J. Yoblinski, M. Stathis and T.F. Guarr, *Inorg. Chem.*, 29 (1990) 1761.

[14] S. van Wallendael and D.P. Rillema, *Coord. Chem. Rev.*, 111 (1991) 297.

[15] M. Furue, M. Naiki, Y. Kanematsu, T. Kushida and M. Kamachi, *Coord. Chem. Rev.*, 111 (1991) 221.

[16] R. Lin and T.F. Guarr, *Inorg. Chim. Acta.*, 167 (1990) 149.

[17] R. Lin, T.F. Guarr and R. Duesing, *Inorg. Chem.*, 29 (1990) 4172.

[18] G. Tapolsky, R. Duesing and T.J. Meyer, *J. Phys. Chem.*, 93 (1989) 3885.

[19] G. Tapolsky, R. Duesing and T.J. Meyer, *Inorg. Chem.*, 29 (1990) 2285.

[20] C.A. Bignozzi, R. Argazzi, C. Chiorboli, S. Roffia and F. Scandola, *Coord. Chem. Rev.*, 111 (1991) 261.

[21] J.R. Schoonover, K.C. Gordon, R. Argazzi, W.H. Woodruff, K.A. Peterson, C.A. Bignozzi, R.B. Dyer and T.J. Meyer, *J. Am. Chem. Soc.*, 115 (1993) 10996.

[22] B.D. Rossenaar, E. Lindsay, D.J. Stufkens and A. Vlček Jr., *Inorg. Chim. Acta*, 250 (1996) 5.

[23] M.W. Kokkes, D.J. Stufkens and A. Oskam, *Inorg. Chem.*, 24 (1985) 4411.

[24] M.W. Kokkes, W.G.J. de Lange, D.J. Stufkens and A. Oskam, *J. Organomet. Chem.*, 294 (1985) 59.

[25] D.L. Morse and M.S. Wrighton, *J. Am. Chem. Soc.*, 98 (1976) 3931.

[26] J.C. Luong, R.A. Faltynek and M.S. Wrighton, *J. Am. Chem. Soc.*, 102 (1979) 1597.

[27] J.C. Luong, R.A. Faltynek and M.S. Wrighton, *J. Am. Chem. Soc.*, 102 (1980) 7892.

[28] R.R. Andréa, W.G.J. de Lange, D.J. Stufkens and A. Oskam, *Inorg. Chem.*, 28 (1989) 318.

[29] H.K. van Dijk, J. van der Haar, D.J. Stufkens and A. Oskam, *Inorg. Chem.*, 28 (1989) 75.

[30] P.C. Servaas, G.J. Stor, D.J. Stufkens and A. Oskam, *Inorg. Chim. Acta*, 178 (1990) 185.

[31] B.D. Rossenaar, F. Hartl and D.J. Stufkens, *Inorg. Chem.*, in press.

[32] B.D. Rossenaar, C.J. Kleverlaan, M.C.E. van de Ven, D.J. Stufkens and A. Vlček, Jr., *Chem. Eur. J.*, 2 (1996) 228.

[33] B.D. Rossenaar, C.J. Kleverlaan, M.C. Stufkens and A. Oskam, *J. Chem. Soc. Chem. Commun.*, (1994) 63.

[34] F.D. Rossenaar, C.J. Kleverlaan, M.C.E. van de Ven, D.J. Stufkens, A. Oskam, K. Goubitz and J. Fraanje, *J. Organomet. Chem.*, 493 (1995) 153.

[35] F.J. García Alonso, A. Llamazares, V. Riera, M. Vivanco, S. García Granda and M.R. Díaz, *Organometallics*, 11 (1992) 2826.

[36] B.D. Rossenaar, M.W. George, F.P.A. Johnson, D.J. Stufkens, J.J. Turner and A. Vlček, Jr., *J. Am. Chem. Soc.*, 117 (1995) 11582.

[37] M.P. Aarnts, D.J. Stufkens, A. Oskam, J. Fraanje and K. Goubitz, *Inorg. Chim. Acta*, in press.

[38] M.P. Aarnts, F. Hartl, K. Peelen, D.J. Stufkens, J. Fraanje, K. Goubitz, M. Wilms, E.J. Baerends and A. Vlček, Jr., *Inorg. Chem.*, 35 (1996) 5468.

[39] M.P. Aarnts, M. Wilms, D.J. Stufkens, E.J. Baerends, I. Clark, M.W. George, J.J. Turner and A. Vlček, Jr., *Chem. Eur. J.*, 2 (1996) 1556.

[40] H.A. Nieuwenhuis, D.J. Stufkens and A. Vlček, Jr., *Inorg. Chem.*, 34 (1995) 3879.

[41] G.F. Strouse, J.R. Schoonover, R. Duesing, S. Boyde, W.E. Jones, Jr. and T.J. Meyer, *Inorg. Chem.*, 34 (1995) 437.

[42] H. Bock and H. tom Dieck, *Chem. Ber.*, 100 (1967) 228.

[43] M.J.A. Kraakman, B. de Klerk-Engels, P.P.M. de Lange, K. Vrieze, W.J.J. Smeets and A.L. Spek, *Organometallics*, 11 (1992) 3774.

[44] H.A. Nieuwenhuis, A. van Loon, M.A. Moraal, D.J. Stufkens, A. Oskam and K. Goubitz, *Inorg. Chim. Acta*, 232 (1995) 19.

[45] H.A. Nieuwenhuis, D.J. Stufkens and A. Oskam, *Inorg. Chem.*, 33 (1994) 3212.

[46] M.J.A. Kraakman, K. Vrieze, H. Kooijman and A.L. Spek, *Organometallics*, 11 (1992) 3760.

[47] H.D. Kaesz, R. Bau, D. Hendrickson and J.M. Smith, *J. Am. Chem. Soc.*, 89 (1967) 2844.

[48] J.M.M. Smits, H. Behm, W.P. Bosman and P.T. Beurskens, *J. Crystallogr. Spectrosc. Res.*, 18 (1991) 447.

[49] N. Walker and D. Stuart, *Acta Crystallogr. Sect. A:*, 39 (1983) 158.

[50] W.H. Zachariasen, *Acta Crystallogr. Sect. A:*, 23 (1967) 558.

[51] A.C. Larson, in F.R. Ahmed, S.R. Hall and C.P. Huber (eds.), *Crystallographic Computing*, Munksgaard, Copenhagen, 1969, pp. 291–294.

[52] D.T. Cromer and J.B. Mann, *Acta Crystallogr. Sect. A:*, 24 (1968) 321.

[53] D.T. Cromer and J.B. Mann, *International Tables for X-Ray Crystallography*, Vol. IV, Kynoch Press, Birmingham, UK, 1974, p. 55.

[54] S.R. Hall, H.D. Flack and J.M. Steward, *XTAL3.2 User's Manual*, Universities of Western Australia, Geneva and Maryland, 1992.

[55] J.L. de Boer and A.J.M. Duisenberg, *Acta Crystallogr. Sect. A:*, 40 (1984) C410.

[56] A.L. Spek, *Acta Crystallogr. Sect. A:*, 46 (1990) C34.

[57] P.T. Beurskens, G. Admiraal, G. Beurskens, W.P. Bosman, S. Garcia-Granda, R.O. Gould, J.M.M. Smits and C. Smykkala,

The *DIRDIF-92 program system, Technical Rep.*, 1992 (Crystallography Laboratory, University of Nijmegen, Netherlands).

[58] G.M. Sheldrick, *SHELXL-93, Program for Structure Refinement*, University of Göttingen, Germany, 1993.

[59] *Grams / 386 implemented in WIN-IR software*, Galactic Industries Corporation and Digilab Division, Bio-Rad Laboratories, 1991–1993.

[60] A. Roland and H. Vahrenkamp, *Chem. Ber.*, *118* (1985) 1133.

[61] H. Zhongli, S. Neferdof, N. Lugan, D. Neilbecker and R. Mathieu, *Organometallics*, *2* (1993) 3837.

[62] A.J. Deeming, M. Karim, N.I. Powell and K.I. Hardcastle, *Polyhedron*, 9 (1990) 623.

[63] E.J. Moore, J.M. Sullivan and J.R. Norton, *J. Am. Chem. Soc.*, *108* (1986) 2257.

[64] M.P. Aarnts, M.P. Wilms, D.J. Stufkens, E.J. Baerends and A. Vlček, Jr., *Inorg. Chim. Acta*, submitted.

[65] J.A. Cabeza, S. Garcia-Granda, A. Llamazares, V. Riera and J.F. van der Maelen, *Organometallics*, *12* (1993) 157.

[66] G.R. Clark, K.R. Flower, W.R. Roper and L.J. Wright, *Organometallics*, *12* (1993) 259.

[67] S.F. Watkins, *J. Chem. Soc. A:*, (1969) 1552.

[68] C.J. Kleverlaan et al., unpublished results.

[69] M.W. Kokkes, T.L. Snoeck, D.J. Stufkens, A. Oskam, M. Christophersen and C.H. Stam, *J. Mol. Struct.*, *131* (1985) 11.

[70] R.A. Burnham and S. Stobart R., *J. Chem. Soc. Dalton Trans*, (1973) 1269.

[71] R.W. Balk, D.J. Stufkens and A. Oskam, *J. Chem. Soc. Dalton Trans.*, (1981) 1124.

[72] R.W. Balk, T. Snoeck, D.J. Stufkens and A. Oskam, *Inorg. Chem.*, *19* (1980) 3015.

[73] G.J. Stor, D.J. Stufkens, P. Vernooijs, E.J. Baerends, J. Fraanje and K. Goubitz, *Inorg. Chem.*, *34* (1995) 1588.

[74] H. tom Dieck, I.W. Renk and K.D. Franz, *J. Organomet. Chem.*, *94* (1975) 417.

[75] G. van Koten and K. Vrieze, *Adv. Organomet. Chem.*, *21* (1982) 151.